Transactions, **SMiRT-26**
Berlin/Potsdam, Germany, July 10-15, 2022
Division II

VERIFICATION OF THE MASTER CURVE CONCEPT (ASTM E1921) FOR THE WELD OF A GERMAN RPV STEEL AT VARIOUS LOADING RATES

Johannes Tlatlik[1]

[1] Fraunhofer IWM, Freiburg, Germany (johannes.tlatlik@iwm.fraunhofer.de)

ABSTRACT

Fracture-mechanical investigations were carried out on the weld metal of a German reactor pressure vessel steel 22NiMoCr3-7. The crack tip loading rate and test temperature were varied in the brittle-ductile transition region, while the results were evaluated using the Master Curve methodology (ASTM E1921), including inhomogeneity analyses. The highly inhomogeneous datasets could be uniformly described with a bimodal distribution function with good accuracy compared to the standard procedure. However, this agreement decreases with crack tip loading rate. The weld metal has a significantly higher toughness than the base material. SEM analysis suggests that the inhomogeneity is due to the stochastic distribution of sharp microcracks, while the observed inhomogeneity is additionally superimposed by dynamic effects (adiabatic heating and local crack arrest) at increased crack tip loading rates. It is argued that the microstructural inhomogeneity is hereby »neutralized« and could instead be interpreted as a possible artifact of the standard Master Curve under dynamic conditions.

INTRODUCTION

The Master Curve methodology is standardized in ASTM E1921 (2021) and used to experimentally determine the temperature-dependent fracture toughness $K_{Jc}(T)$ of ferritic steels. Because brittle failure must be excluded in safety-relevant nuclear components, reactor pressure vessel (RPV) steels are commonly assessed with this concept. The concept is macroscopic and allows a probabilistic description of the experimental scatter in K_{Jc}-values via a three-parametric Weibull distribution. The physical reason for this scatter is linked to the statistical distribution of cleavage-inducing brittle particles in the microstructure. The empirically derived shape factor of the Master Curve is assumed constant with $p = 0.019$ /°C. The toughness of the material is characterized by a single parameter, the reference temperature T_0, which shifts the Master Curve along the temperature axis.

The concept predominantly deals with quasi-static testing conditions, but elevated loading rates are addressed by Annex A1 of ASTM E1921 (2021) and A14 of ASTM E1820 (2020). Recently, extensive research has shown that for the German RPV steel 22 NiMoCr3-7 (A508 Grade 2, Cl 1), the Master Curve methodology can show severe shortcomings at elevated loading rates of approximately 10^3 to 10^5 MPa√m/s. Exemplary publications on this topic include Mayer et al. (2017, 2012), Reichert et al. (2016, 2017), Schindler and Kalkhoff (2015), and Tlatlik and Reichert (2017). The embrittling effect of the elevated loading caused a shift of the Master Curve to higher temperatures, resulting in higher T_0-values, but it was also found that the Master Curve was too flat for higher fracture toughness values greater than 100 MPa√m and test temperatures significantly higher than $T > T_0$. The fracture probability can be significantly overestimated compared to comprehensive experimental data in some cases. Moreover, there is strong reason to believe that the shape of the Master Curve with $p = 0.019$ /°C and the underlying Weibull distribution appear to be unsuitable under these conditions. Essentially, this phenomenon can be explained by the strong temperature increase in the crack tip region, whereby a general adjustment of $p = 0.030$ /°C

leads to significantly improved results for elevated loading rates, Tlatlik and Reichert (2017), Tlatlik (2017b). However, it was also observed that the underlying Weibull distribution function selected here also changes under increased load rates, and so adjusting the slope of the Master Curve is not sufficient to adequately describe the probability of failure. Local crack arrest along the crack front was identified as a key reason for this Tlatlik (2017a), which shifts global failure towards higher fracture toughness values.

The material discussed, however, was very homogeneous. This paper deals with further investigations involving a weld of the RPV steel at quasi-static and elevated loading rates that shows significant material inhomogeneity, which is addressed by Annex X5 of ASTM E1921 (2021). The fracture mechanics tests are analyzed and evaluated with the proposed methods of Annex X5 and evaluated in the context of the described shortcomings of the Master Curve methodology under elevated loading rates.

MATERIAL

The test material was a weld metal of the ferritic-bainitic RPV steel 22NiMoCr3-7 (A508 Grade 2, Cl 1) from the vessel intended for the Biblis C plant, which was never used. An overview of measured common mechanical properties is presented in Table 1. Side-grooved (10 %) SE(B)40x20 specimens with a length of 220 mm were extracted from the weld like seen in Figure 1. The specimens were fatigue-precracked to a crack length ratio of $a_0/W = 0.5$, according to the procedure outlined in ASTM E1921 (2021). More details about the specimens can be obtained from Mayer et al. (2017).

Hardness measurements of the weld metal showed an almost constant hardness profile over a large range of about 20 to 220 mm of the wall thickness, which was used for specimen extraction to avoid unnecessary material inhomogeneity and scatter. Four layers (A: outside, B, C, D: inside) were defined in which the subsequent crack propagation is directed in radial direction of the RPV (T-S-orientation).

Table 1: Overview of common mechanical properties of the weld material at RT (T in °C)

R_{eL} [MPa]	R_m [MPa]	A [%]	T_{28J} [°C]	T_{41J} [°C]	$T_{50\%US}$ [°C]	E(T) [MPa]
557	643	29.3	-66	-58	-34	211093 - 51 T

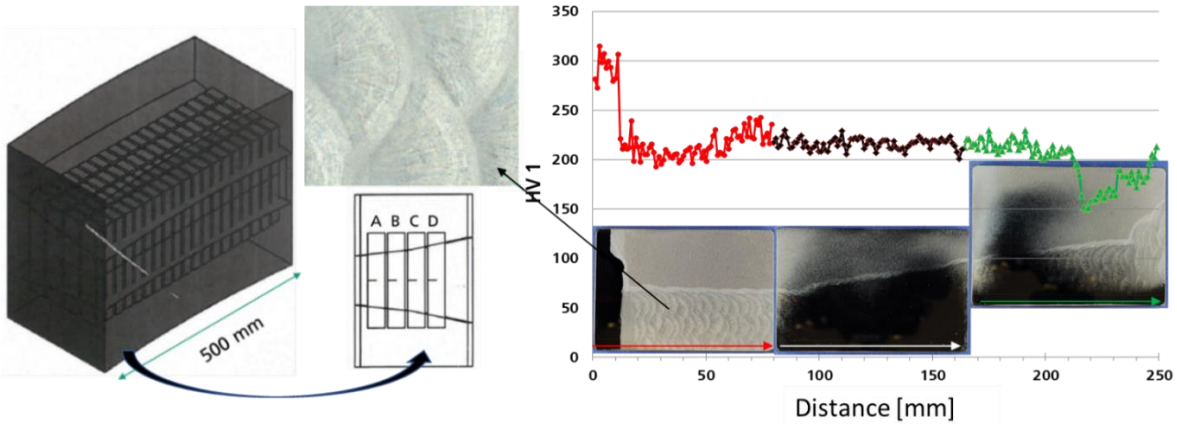

Figure 1. Overview of specimen extraction from the vessel wall and hardness measurement

TESTING

Quasi-static and dynamic fracture mechanics tests were carried out on a servo-hydraulic 500 kN high-speed tensile test machine with a three-point bending setup in accordance with annex A14 of ASTM E1820 (2020b). Testing took place in the range of $1x10^0$ MPa$\sqrt{m}$/s $\leq dK/dt \leq$ $1x10^4$ MPa$\sqrt{m}$/s in the ductile to brittle transition region of the material. The database includes eight test series at $1x10^0$, $1x10^2$, $1x10^3$ and

$1x10^4$ MPa√m/s in the temperature range -100 °C to -20 °C, each with 9 to 22 samples. The highest striker velocities of 90 mm/s used here can be classified as moderately elevated loading rates and show only minor inertial effects, so that an external force measurement with a piezo quartz load cell delivered sufficiently good measurement signals in all cases. In all cases the test time t_0 was greater than the minimum allowable test time t_w defined in ASTM E1820 (2020b), annex A14. Crack mouth opening displacement CMOD for the SE(B)-specimens was measured using a clip-gauge for loading rates $dK/dt \leq 10^2$ MPa√m/s and via high-speed camera for $dK/dt \geq 10^3$ MPa√m/s. Digital image correlation was used to obtain the local displacements at the specimen edge. Cooling of the specimens was carried out in a temperature chamber with gaseous nitrogen, with the temperature of the specimens being controlled locally by a thermocouple at the specimen. More details about the testing procedure can be obtained from Mayer et al. (2017).

EVALUATION AND INHOMOGENEITY ANALYSIS

Standard Master Curve Methodology

The fracture-mechanical properties K_{Jc} and $K_{Jc,d}$ (subscript d for dynamic) were evaluated according to ASTM E1921 (2021) with reference to ASTM E1820 (2020b) by determining the elastic and plastic parts of the J-integral, assuming a plane strain condition until instability. The crack tip loading rate dK/dt was calculated according to ASTM E1820 (2020b) using the quotient of $K_{Jc,d}$ and the time at fracture t_f. The determined fracture toughness values were normalized to a standard thickness of 25.4 mm (1T), resulting in $K_{Jc,d(1T)}$. The probability of failure P_f is determined with a three-parameter Weibull distribution

$$P_f(K_J) = 1 - exp\left[-\left(\frac{K_J - K_{min}}{K_0 - K_{min}}\right)^m\right] \quad (1)$$

with the empirically determined constant K_{min} = 20 MPa√m, the Weibull modulus m = 4 and the scale parameter K_0. The postulated constant temperature dependency of the median fracture toughness curve $K_{Jc,med}$ for ferritic steels is defined as

$$K_{Jc,med} = 30 + 70\ exp[0.019(T - T_0)] \quad (2)$$

with the Master Curve reference temperature T_0, defined as the temperature at which the median fracture toughness curve $K_{Jc,med}$ has a fracture toughness of 100 MPa√m. K_0 is determined so that Equation (2) is satisfied. The value p = 0.019 /°C in equation (2) describes the slope of the temperature-dependent fracture toughness curve and satisfactorily describes the behavior of most ferritic steels under quasi-static loads with homogenic material. The evaluation can be carried out using one test series at one test temperature or by a multi-temperature evaluation with several series and temperatures.

Inhomogeneity Analysis

Appendix X5 of ASTM E1921 (2021) describes the treatment of potentially inhomogeneous data sets or material properties. First, the data set is checked for macroscopic homogeneity using the SINTAP method, Wallin (2012), after which, if the criterion is violated, the inhomogeneity can be examined using other analysis methods. Initially, all $K_{Jc(1T)}$-values above the median fracture toughness curve $K_{Jc,med}$ of a dataset are censored to the corresponding values of $K_{Jc,med}(T)$. The new dataset is used to calculate a new $T_{0,step\ 2}$. This procedure is repeated until the criterion $T_{0,step\ n} - T_{0,step\ n-1} < 0.5$ is fulfilled, i.e. a nearly constant value for the reference temperature is determined. The dataset is assumed to be potentially inhomogeneous if

$$T_{0,scrn} - T_{0,step\ 1} \leq 1{,}44\sqrt{\beta^2/r} \quad (3)$$

with the reference temperature $T_{0,scrn}$ (scrn: screen), the sample size uncertainty factor β, and the total number of uncensored data r is not fulfilled in the last iteration step. In the case of inhomogeneity, three alternative evaluation methods are proposed: the simplified, bimodal, and multimodal method. For details, the reader is referred to Appendix X5 of ASTM E1921 (2021).

The simplified method provides a conservative alternative reference temperature T_{0IN} or a lower limit curve for the potentially inhomogeneous data set, instead of the conventional T_0-value. This is particularly useful for small data sets ($N \leq 9$), where potential macroscopic inhomogeneity cannot be accurately determined.

Data sets with at least 20 data points enable a more precise determination and description of potentially inhomogeneous data sets. A bimodal distribution function applies to data sets with two toughness populations, A and B. Typical examples of this are examinations of specimens taken from heat-effected zones. The distribution of two reference temperatures (T_A and T_B) and the probability of a data point belonging to the respective populations (p_A and p_B) are described. The more brittle of the two populations is defined as population A, so that the following applies: $T_B \leq T_A$.

A minimum of 20 data points also allows the use of a multimodal fracture toughness distribution function. This describes a data set with several randomly distributed fracture toughness populations, which are typically caused by randomly distributed microstructures in the material. The individual populations in the overall data set follow an individual Master Curve Weibull distribution that belongs to an overall distribution. The mean reference temperature T_m of all populations and the standard deviation σ_{TM} of the median fully define the distribution function.

RESULTS

Quasi-static testing conditions at dK/dt = 1x10^0 MPa√m/s are discussed first with the aid of Figure 2, which shows the Master Curve evaluation of the standard, bimodal and multimodal method. This dataset is by far the most extensive, as can be seen in Table 2. At a first glance, the standard multi-temperature evaluation with T_0 = -100 °C shows a decent agreement with the single-temperature analysis of the individual test series, but the data is better described by the inhomogeneity analysis and the corresponding alternative distributions, especially considering the 5 % curve. The calculated alternative reference temperatures are T_A = -80 °C, T_B = -113 °C, T_M = -90 °C and T_{0IN} = -87 °C which makes apparent that the standard T_0-value overestimates the toughness of the material. However, the methodology does not allow any statement about the nature or affiliation of the data set to a specific distribution, which can only be deduced based on the physical background of the material (production, extraction, etc.). This topic will be examined later in more detail. In absence of a physical background, the ASTM E1921 (2021) standard recommends the evaluation that produces the most conservative results, here T_A = -80 °C.

Figure 5 a) shows the cumulated probability of failure P_f of the Master Curve as a function of $K_{Jc,d(1T)}$ in order to analyze the underlying distribution function, which was calculated by the equation

$$P_f = \frac{-1}{exp\left\{\left(\frac{K_{J(1T)-20}}{11+77\exp\left[p(T-T_0)\right]}\right)^4\right\}} + 1 \qquad (4)$$

The rank probability $z(P)$ for experimental data was calculated for the confidence level P of the i^{th} data point of N tests by solving the equation from Wallin (1989):

$$1 - \sum_{k=1}^{i} \frac{N!}{(k-1)!(N-k+1)!} z^{k-1}(1-z)^{N-k+1} = P \qquad (5)$$

An approximation for the median rank probability with a confidence level of 50 % can be expressed by

$$P_{f(50\%)} = (i - 0.3)/(N + 0.4) \qquad (6)$$

and compared to the sorted $K_{Jc,d(1T)}$-values in ascending order. In addition, the 5 % and 95 % confidence bounds of the measured rank probability are calculated and included in the figures. The solid line represents the standard evaluation for the multi-temperature analysis. It is apparent, that the distribution of the standard evaluation describes the data poorly for the series tested at T = -100 °C while taking into account the error bars. Most importantly, the assessment is non-conservative here, whereas the agreement is better for T = -60 °C. The bimodal and multimodal analysis, on the other hand, produce much better results, especially in terms of conservatism. The »dynamic« evaluation with the adjusted shape factor p = 0.03 /°C is included in Figure 2 and Figure 5 a) only for informational purposes and does not provide a good assessment of the material's fracture behavior at quasi-static testing conditions. Considering the distributions in Figure 5 a), it is apparent that the bimodal and multimodal analysis provide an overall better agreement with the experimental results under quasi-static conditions compared to the standard evaluation.

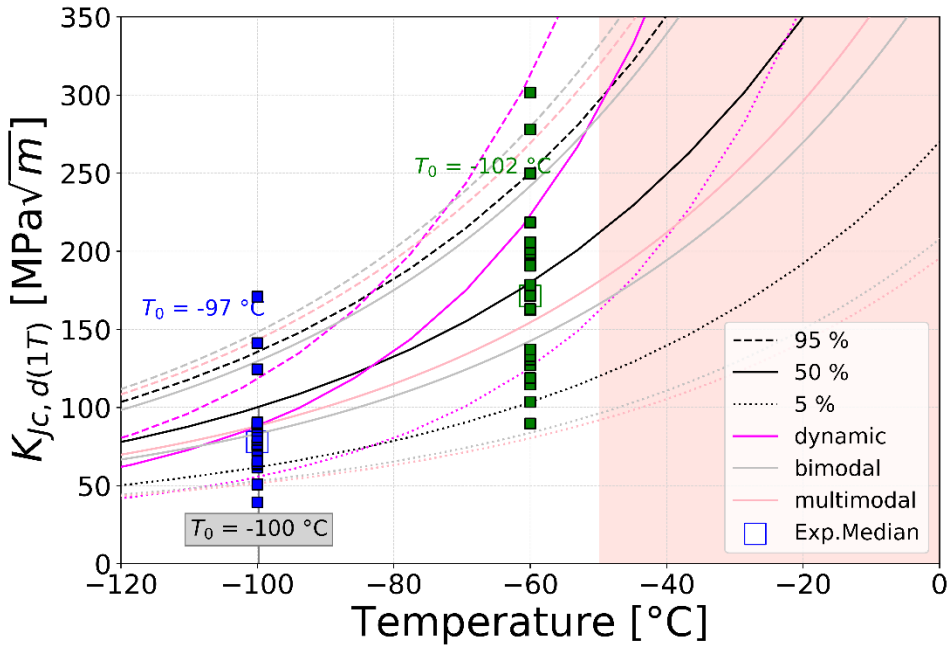

Figure 2. Master Curve evaluations for dK/dt = 1x10^0 MPa√m/s

Slightly elevated loading rates of dK/dt = 1x10^2 MPa√m/s are depicted in Figure 3 and Figure 5 b). The dataset was also detected to be inhomogeneous. The single-temperature T_0-values of the standard method diverge quite strongly from the multi-temperature evaluation. The use of the bimodal and multimodal distributions provides a better assessment for the series tested at T = -80 °C, whereas for T = -40 °C the agreement appears to be slightly worse compared to the standard method. However, the lower bound of the curve appears to be significantly more appropriate and conservative. The »dynamic« evaluation with p = 0.03 /°C assesses fracture behaviour quite well for T = -80 °C but overestimates toughness for T = -40 °C, especially for lower load levels.

The data of the moderately elevated loading rates of dK/dt = 1x10^3 MPa√m/s showed no signs of inhomogeneity. Therefore, only the standard and »dynamic« evaluation was performed here, whereas the data is only discussed by Figure 5 c). It is noteworthy, however, to mention that the dataset becomes inhomogeneous if additional data from an ASTM interlaboratory study is included. Both predicted probabilities of failure P_f lie within the 5 % and 95 % confidence bounds of the measured rank probability and show similar agreement with the experimental data. However, the predicted median $K_{Jc,med}$ is in better agreement with the experimental values for both test series when using the »dynamic« evaluation.

The results regarding the elevated loading rates at dK/dt = 1x10^4 MPa√m/s are shown in Figure 4 and Figure 5 d). The dataset is inhomogeneous. It is apparent that the standard Master Curve evaluation overestimates toughness at T = -60 °C, while the bimodal and multimodal distributions provide a better agreement with the experimental data, but the probability of failure is barely within the 5 % and 95 % confidence bounds. The »dynamic« evaluation shows the best agreement here. The experiments at T = -20 °C are described decently by the standard evaluation, but toughness is significantly underestimated by the alternative bimodal and multimodal distributions. The »dynamic« evaluation, like the data at T = -60 °C, accurately describes the data for T = -20 °C.

Furthermore, the probability of a data point belonging to either of the populations A and B was calculated for the bimodal distribution for all datasets. It was observed that the association of a data point p_A with the more brittle population A is consistently more likely than with the population B (see Table 2). Conclusively, the inhomogeneity is caused by the occurrence of a less likely, tougher population or microstructure within the weld.

To summarize, the agreement of the bimodal and multimodal distributions with the experimental data is quite good for quasi-static testing conditions for the examined weld material and provides a better alternative to the standard Weibull distribution, especially since the latter overestimates the material's toughness in terms of reference temperature. However, the agreement of these alternative distribution functions appears to systematically decrease with increasing loading rate dK/dt. Contrary to this, the quality of the »dynamic« evaluation with p = 0.03 /°C increases with dK/dt. A summary of all evaluated data can be seen in Table 2.

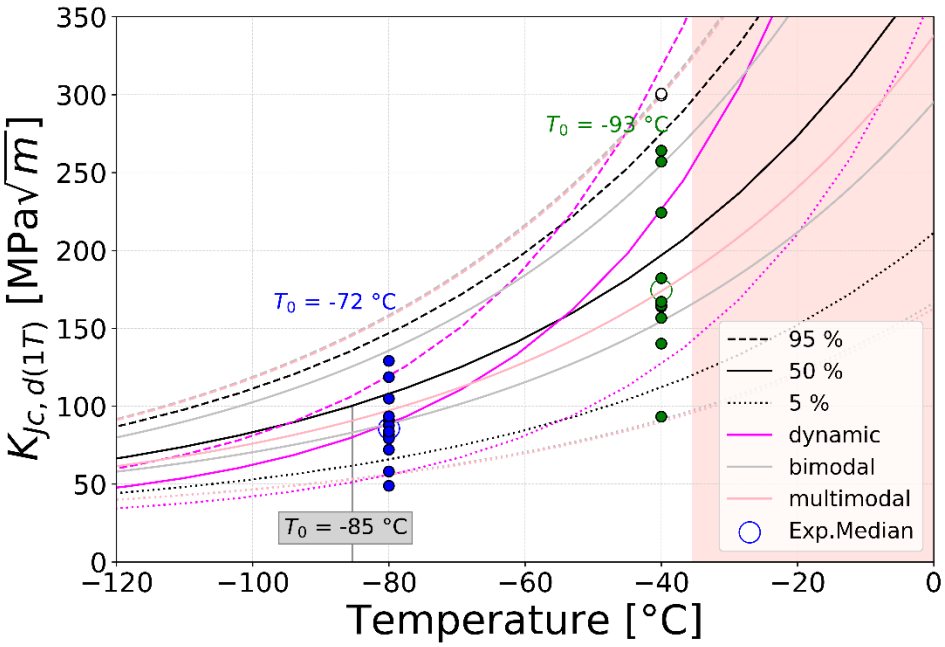

Figure 3. Master Curve evaluations for dK/dt = 1x10^2 MPa√m/s

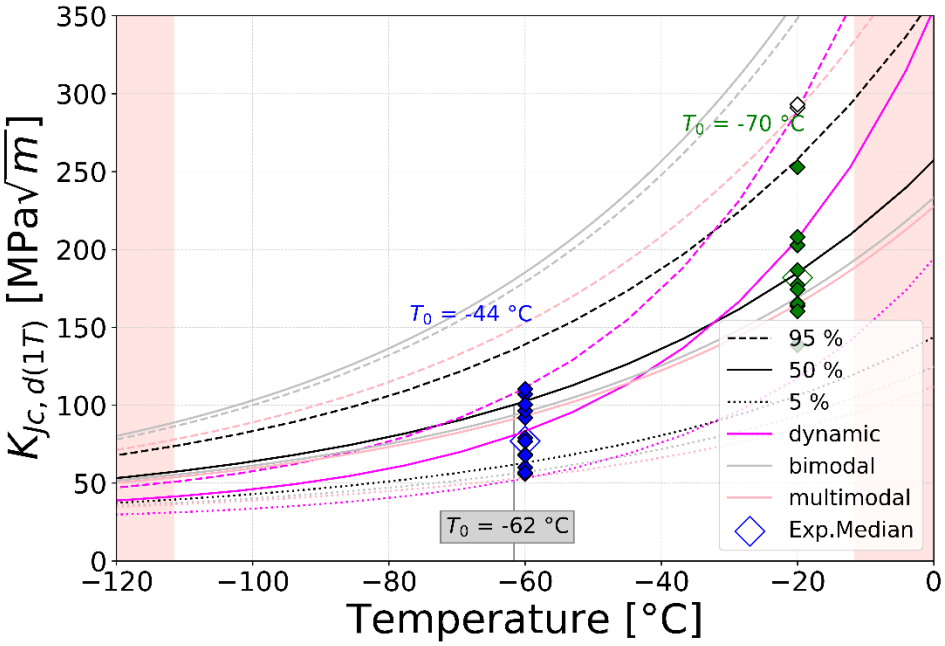

Figure 4. Master Curve evaluations for dK/dt = 1x10^4 MPa√m/s

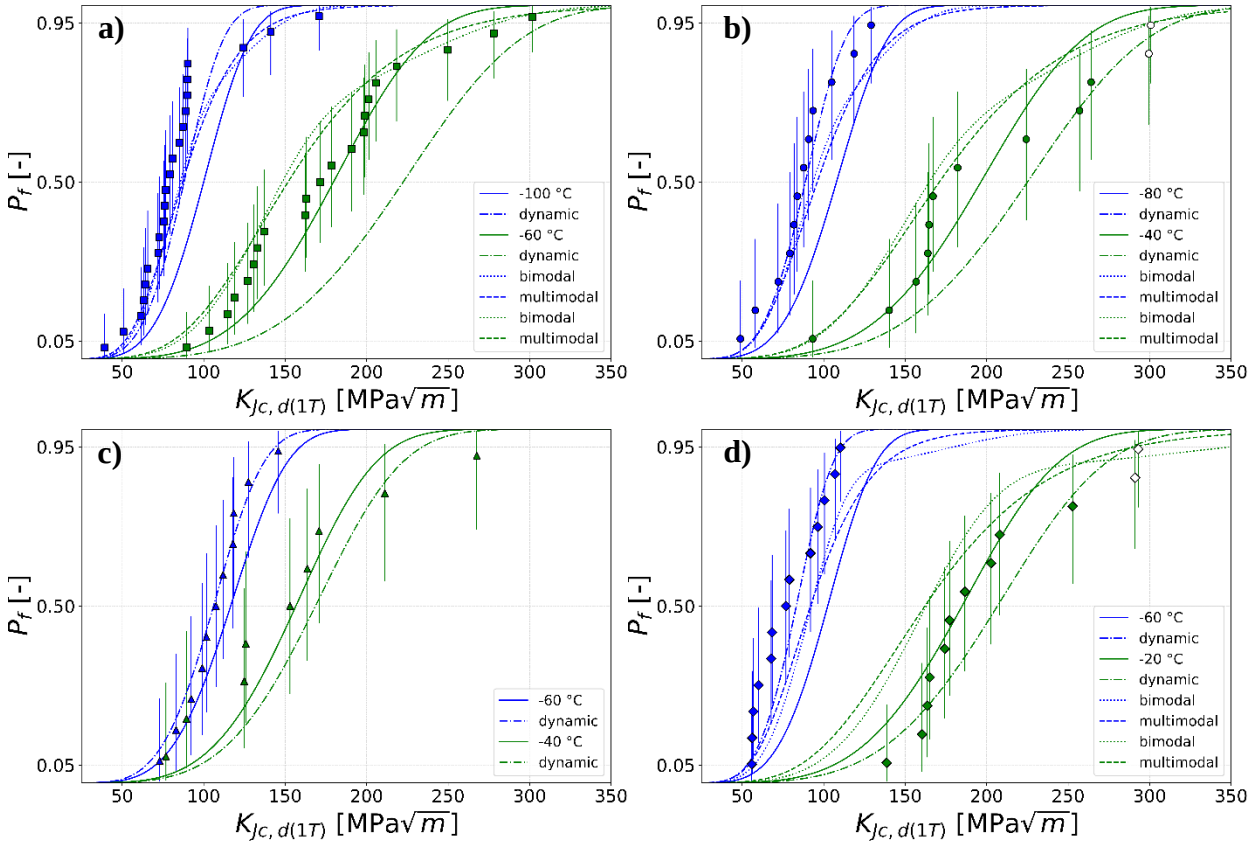

Figure 5. Calculated and measured probability of failure by multi-temperature method a) 1x10^0 MPa√m/s, b) 1x10^2 MPa√m/s, c) 1x10^3 MPa√m/s, d) 1x10^4 MPa√m/s

Table 2: Overview of all experiments and evaluations

T [°C]	log(dK/dt) [MPa√m/s]	No. of Tests [-]	$T_{0,sing}$ [°C]	$T_{0,multi}$ [°C]	$T_{o,sing}^{dyn}$ [°C]	$T_{o,multi}^{dyn}$ [°C]	T_{0IN} [°C]	T_A [°C]	T_B [°C]	T_M [°C]	p_A [-]
-100	0	22	-97	-100	-98	-94	-87	-80	-113	-90	0.673
-60	0	21	-102		-87						
-80	2	12	-72	-85	-75	-74	-72	-65	-96	-78	0.610
-40	2	12	-93		-73						
-60	3	10	-64	-71	-62	-63	N.A.	N.A.	N.A.	N.A.	N.A.
-40	3	9	-76		-63						
-60	4	13	-44	-62	-50	-51	-54	-51	-97	-55	0.85
-20	4	12	-70		-52						

ANALYSIS OF EXTRACTION LOCATION AND FRACTURE SURFACES

The aim of the analysis of the extraction position and fracture surfaces was to obtain physical reasons for the observed scattering of the fracture toughness, so that they can be used in the inhomogeneity analysis with regard to the choice of a physically based distribution function. The graphical representation of the specimen positions can be seen in Figure 1. A slight tendency towards an increase in fracture toughness from the outer wall of the container inwards (layer D → A) was observed, but this is superimposed by strong scatter. A grouping of the specimens and subsequent inhomogeneity analysis was performed, however, the grouped datasets still showed signs of inhomogeneity. Consequently, the extraction location could not be used to interpret the material inhomogeneity.

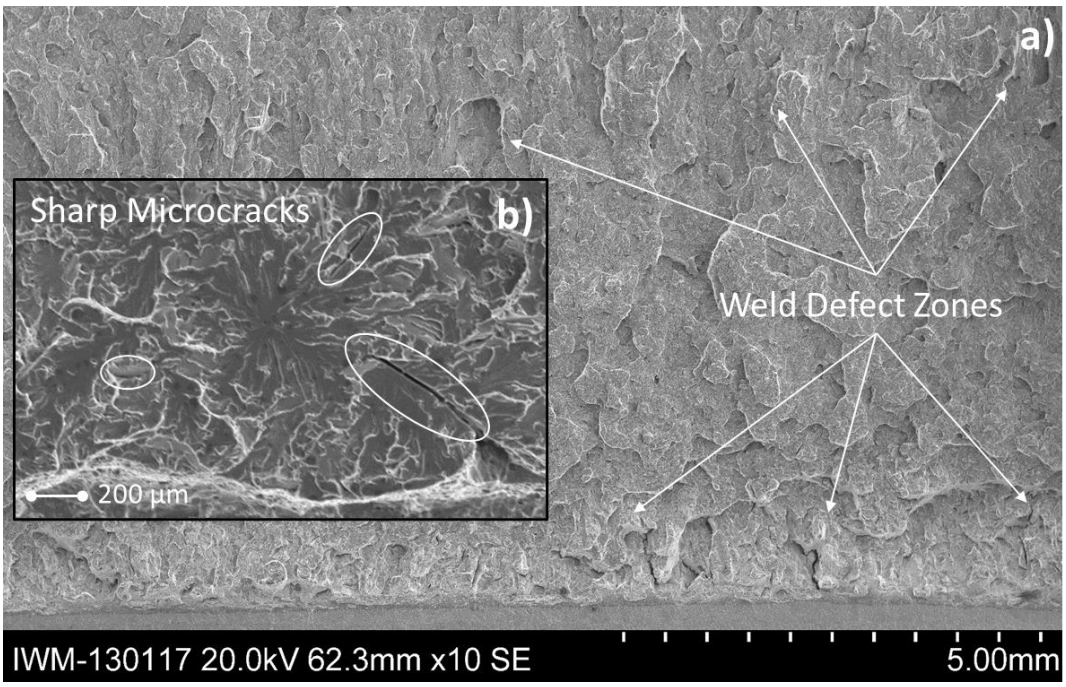

Figure 6. SEM-images: a) crack tip region shows periodic weld defect zones ($K_{Jc,d(1T)}$ = 211.1 MPa√m), b) sharp cracks at initiation site ($K_{Jc,d(1T)}$ = 77.1 MPa√m), both specimens with dK/dt = 1x10^3 MPa√m/s

Furthermore, SEM images of selected fracture surfaces were taken in order to find local microstructural reasons for the scattering of the measured values. Periodically arranged weld defect zones

with a width of several hundred micrometers were observed occurring every 5 mm on all specimens (see Figure 6 a)). The position of these very large welding defects in relation to the initial crack front could not be linked to the fracture toughness. In the case of specimens with very low fracture toughness values, as shown in Figure 6 b), very sharp cracks were often found in the immediate vicinity of the fracture origins, which may have the effect of triggering cleavage. The inhomogeneity could thus be attributed to the stochastic distribution of the sharp microcracks in the crack tip region. Considering the calculated high probability p_A for an assumed bimodal distribution, the inhomogeneity in turn appears to be caused by material volume with very low quantities of these sharp cracks, which is statistically less likely to occur. However, more extensive SEM investigations must confirm this assumption to be sure.

Furthermore, a similar number of local crack arrest events was discovered on the fracture surfaces of the weld metal as in the base material (see Tlatlik (2017a), which have a significant impact on the distribution of the fracture toughness values at elevated loading rates.

DISCUSSION OF PHYSICAL BACKGROUND

As recent publications like Mayer et al. (2017, 2012), Reichert et al. (2016, 2017), Schindler and Kalkhoff (2015), Tlatlik and Reichert (2017), Tlatlik (2017a, 2017b) have demonstrated, the Master Curve methodology shows considerable shortcomings at elevated loading rates for the base material 22 NiMoCr3-7. Adiabatic heating was found to impact fracture behavior at loading rates $dK/dt \geq 10^3$ MPa$\sqrt{}$m/s, whereas local crack arrest was observed at local temperatures $T \geq$ -20 °C, especially for testing temperatures $T > T_0$. These mechanisms were found to be associated with a significant increase in fracture toughness, accompanied by a strong compression of the distribution of the fracture toughness values compared to quasi-static testing. Both mechanisms were identified to be relevant in similar magnitude for the RPV weld as well. On the other hand, the observed inhomogeneity has its roots in local microstructural differences, which results in precisely the opposite: a widening of the distribution (see especially Figure 2). The inhomogeneity is thus superimposed by the dynamic effects, so that the components cannot be considered individually.

The observations are interpreted in such a way that the dynamic effects counteract the effects of the microstructural inhomogeneities, and the observed inhomogeneity is an artifact of the shortcomings of the standard Master Curve at elevated loading rates. The statistical implications of the material inhomogeneity here are thus »neutralized« by compressing the distribution function, while the »dynamic« Master Curve with $p = 0.03$ /°C becomes much more suitable as the load rate, and therefore the dominance of the dynamic effects, increases. This interpretation is strengthened by the fact that under quasi-static conditions, the Master Curve with $p = 0.03$ /°C shows only poor agreement. Most importantly, if the inhomogeneity analysis of the datasets at elevated loading rates is instead performed with $p = 0.03$ /°C, then inhomogeneity disappears.

As a result, it is recommended to test near or below T_0 to minimize the influence of the dynamic effects and a possible non-conservative assessment. This simple recommendation avoids an extensive adjustment of the ASTM E1921 (2021) standard, which is far too complex to account for all of the impacts at elevated loading rates.

CONCLUSION

The following most important conclusions can be extracted from this work:

- According to ASTM E1921 Annex X5, the analysis of the weld metal showed strong inhomogeneity of the data sets. SEM-analysis suggests that the inhomogeneity is due to the stochastic distribution of sharp microcracks.
- Bimodal and multimodal distributions provide an improved and more conservative description of the fracture behavior, especially under quasi-static conditions.
- Conservatism of the bimodal and multimodal distributions increases, but general agreement with the experimental data decreases systematically with increasing loading rate dK/dt.

- T_A gives the most conservative result in all cases and is recommended by ASTM E1921 as the reference temperature.
- The material inhomogeneity is »neutralized« with increasing loading rate since dynamic effects (adiabatic heating and local crack arrest) counteract the resulting statistical implications.
- It is recommended to test near or below T_0 to minimize the influence of the dynamic effects and a possible non-conservative assessment.

ACKNOWLEDGEMENT

The research project "Analysis of the Master Curve Concept at Elevated Loading Rates" was funded by the German Federal Ministry for the Environment, Nature Conservation, Nuclear Safety and Consumer Protection (Project No. 1501563A) on basis of a decision by the German Bundestag.

Supported by:
Federal Ministry
for the Environment, Nature Conservation,
Nuclear Safety and Consumer Protection
based on a decision of
the German Bundestag

REFERENCES

ASTM Standard E1921-21 (2021); "Standard test method for determination of reference temperature T_0 for ferritic steels in the transition range", ASTM International, West Conshohocken, PA, USA.

ASTM Standard E1820-20b (2020); "Standard Test Method for Measurement of Fracture Toughness", ASTM International, West Conshohocken, PA, USA.

Mayer, U. (2012); "Determination of Dynamic Fracture Toughness at High Loading Rates", *Proceedings of the ASME 2012 International Mechanical Engineering Congress & Exposition*, IMECE2012-85383, Houston, Texas, USA, November 9-15.

Mayer, U., Reichert, T., Tlatlik, J. (2017); "Fracture Mechanics at Elevated Loading Rates in the Ductile to Brittle Transition Region", *Proceedings of the ASME 2017 Pressure Vessels and Piping Conference*, PVP2017-65358, July 16-20, 2017, Waikoloa, Hawaii, USA.

Reichert, T., Böhme, W. and Tlatlik J. (2016); "Modified Shape of Dynamic Master Curves due to Adiabatic Effects", *21st European Conference on Fracture*, ECF21, 20-24 June 2016, Catania, Italy.

Reichert, T., Tlatlik, J. (2017); "Influence of Local Temperature and Local Crack Arrest Phenomena on Dynamic Fracture Toughness", *14th International Conference on Fracture (ICF 14)*, June 18-23, 2017, Rhodes, Greece.

Schindler, H. and D. Kalkhof (2015); "A Closer Look at Effects of the Loading Rate on Fracture Toughness in the Ductile-to-Brittle Transition Regime of a Ferritic Steel", *Journal of Testing and Evaluation*, Vol. 43, No. 3, pp. 507-516.

Tlatlik, J. (2017a); "Investigation of Cleavage Fracture Under Dynamic Loading Conditions: Part I Fractographic Analysis", *Engineering Fracture Mechanics*, 184, 39-50.

Tlatlik, J. (2017b); "Investigation of Cleavage Fracture Under Dynamic Loading Conditions: Part II Numerical Analysis", *Engineering Fracture Mechanics*, 184, 22-38.

Tlatlik, J., Reichert, T. (2017); "Correlation of Fractographic Examinations with Numerical Calculations Regarding Dynamic Fracture", *2017 ASME Pressure Vessels & Piping Conference*, 16-20 2017, Waikoloa, Hawaii, USA.

Wallin, K. (1989); "Optimized estimation of the Weibull distribution parameters", VTT Research Reports 604.

Wallin, K. (2012); "Inhomogeneity Screening Criterion for the ASTM E1921 To Estimate Based on the SINTAP Lower-Tail Methodology", *Journal of Testing and Evaluation*, Vol. 40, No. 6.